Original Article

Loss-of-Function Mutation in Toll-Like Receptor 4 Prevents Diet-Induced Obesity and Insulin Resistance

Daniela M.L. Tsukumo,[1] Marco A. Carvalho-Filho,[1] José B.C. Carvalheira,[1] Patrícia O. Prada,[1] Sandro M. Hirabara,[2] André A. Schenka,[3] Eliana P. Araújo,[1] José Vassallo,[3] Rui Curi,[2] Lício A. Velloso,[1] and Mario J.A. Saad[1]

Obesity is associated with insulin resistance and a state of abnormal inflammatory response. The Toll-like receptor (TLR)4 has an important role in inflammation and immunity, and its expression has been reported in most tissues of the body, including the insulin-sensitive ones. Because it is activated by lipopolysaccharide and saturated fatty acids, which are inducers of insulin resistance, TLR4 may be a candidate for participation in the cross-talk between inflammatory and metabolic signals. Here, we show that C3H/HeJ mice, which have a loss-of-function mutation in TLR4, are protected against the development of diet-induced obesity. In addition, these mice demonstrate decreased adiposity, increased oxygen consumption, a decreased respiratory exchange ratio, improved insulin sensitivity, and enhanced insulin-signaling capacity in adipose tissue, muscle, and liver compared with control mice during high-fat feeding. Moreover, in these tissues, control mice fed a high-fat diet show an increase in IκB kinase complex and c-Jun NH_2-terminal kinase activity, which is prevented in C3H/HeJ mice. In isolated muscles from C3H/HeJ mice, protection from saturated fatty acid–induced insulin resistance is observed. Thus, TLR4 appears to be an important mediator of obesity and insulin resistance and a potential target for the therapy of these highly prevalent medical conditions. *Diabetes* 56:1986–1998, 2007

Insulin resistance in obesity and type 2 diabetes is associated with an abnormal inflammatory state. In addition, during the last decade, we have seen great progress in this field attributable to the identification of several downstream mediators and signaling pathways that provide cross-talk between inflammatory and metabolic signaling (1–9).

Toll-like receptors (TLRs) play a critical role in the activation of innate immune responses in mammals by recognizing conserved pathogen-associated molecular patterns (10–12). To date, 13 members of the TLR family have been identified in mammals. TLR4 is a subclass of TLRs that can be activated by lipopolysaccharide (LPS) and by nonbacterial agonists, such as saturated fatty acids (13,14). The activation of TLR4 signaling induces upregulation of intracellular inflammatory pathways related to the induction of insulin resistance, such as c-Jun NH_2-terminal kinase (JNK) and IκB kinase complex (IKKβ)/inhibitor of nuclear factor-κB (IκBα)/nuclear factor-κB (NF-κB) (10). However, the role of TLR4 in the cross-talk between inflammatory and metabolic signaling has not yet been investigated. Here, we show that mice with a loss-of-function mutation in TLR4 (C3H/HeJ) are protected against the development of diet-induced obesity and insulin resistance and that, in isolated muscles from C3H/HeJ mice, there is a protection from saturated fatty acid–induced insulin resistance.

RESEARCH DESIGN AND METHODS

Male C3H/HeJ, C3H/HeN, and C57Black/10ScNC mice and their respective controls were obtained from The Jackson Laboratory and provided by the University of São Paulo. The mice were bred under specific pathogen-free conditions at the Central Breeding Center of University of Campinas. All antibodies were from Santa Cruz Technology (Santa Cruz, CA), except anti-pAkt, which was from Cell Signaling Technology (Beverly, MA), anti–phospho-insulin receptor substrate-1 (IRS-1)^{Ser307} was obtained from Upstate Biotechnology (Lake Placid, NY), and anti-F4/80 was from Abcam. Routine reagents were purchased from Sigma Chemical (St. Louis, MO), unless otherwise specified.

All experiments were approved by the ethics committee at the State University of Campinas. Six-week-old male C3H/HeJ mice and their controls (C3H/HeN) were divided into two groups with similar body weights and assigned to receive two kinds of diet: a standard rodent chow and water ad libitum or a high-fat diet (HFD) consisting of 55% calories from fat, 29% from carbohydrate, and 16% from protein. Body weight and food intake were measured weekly. Glucose tolerance tests and insulin tolerance tests were performed on these mice after 8 weeks of consumption of the diets, as described previously (2,15).

Assays. Leptin, insulin, and adiponectin concentrations were determined by an enzyme-linked immunosorbent assay (ELISA) (Linco). Serum free fatty acid (FFA) levels were analyzed using NEFA-kit-U (Wako Chemical, Neuss,

From the [1]Department of Internal Medicine, State University of Campinas, Campinas, São Paulo, Brazil; the [2]Department of Physiology and Biophysics, Institute of Biomedical Sciences, University of São Paulo, São Paulo, Brazil; and the [3]Department of Pathology, State University of Campinas, Campinas, São Paulo, Brazil.

Address correspondence and reprint requests to Mario J.A. Saad, MD, Departamento de Clínica Médica, FCM-UNICAMP, Cidade Universitária Zeferino Vaz, Campinas, SP, Brazil, 13081-970. E-mail: msaad@fcm.unicamp.br.

Received for publication 14 November 2006 and accepted in revised form 18 May 2007.

Published ahead of print at http://diabetes.diabetesjournals.org on 22 May 2007. DOI: 10.2337/db06-1595.

CLS, crown-like structure; ELISA, enzyme-linked immunosorbent assay; FFA, free fatty acid; HFD, high-fat diet; IGTT, intraperitoneal glucose tolerance test; IκBα, inhibitor of nuclear factor-κB; IKKβ, IκB kinase complex; IL, interleukin; IR, insulin receptor; IRS-1, insulin receptor substrate-1; JNK, c-Jun NH_2-terminal kinase; LPS, lipopolysaccharide; NK-κB, nuclear factor-κB; RER, respiratory exchange ratio; TNF, tumor necrosis factor; TLR, Toll-like receptor; WAT, white adipose tissue.

Germany) with oleic acid as a standard. Glucose values were measured from whole venous blood with a glucose monitor (Glucometer; Bayer). We determined serum concentrations of interleukin (IL)-6 and tumor necrosis factor (TNF)-α using Mouse IL-6 ELISA and Mouse TNF-α ELISA (Pierce Endogen, Rockford, IL).

Light microscopy. Mice were fasted for 12 h and killed with an overdose of anesthetic (sodium thiopental). Epididymal white adipose tissue (WAT) depots were dissected and assessed by light microscopy, morphometry, and transmission electron microscopy. After dissection, WAT depots were fixed by immersion in 4% formaldehyde in 0.1 mmol/l phosphate buffer, pH 7.4, for <24 h, dehydrated, cleared, and then embedded in paraffin. Serial sections (5-μm thick) were obtained and then stained by hematoxylin and eosin to assess morphology.

Morphometry. Tissue sections were observed with a Zeiss Axiophot light microscope using a ×40 objective, and digital images were captured with a Canon PowerShot G5. Crown-like structure (CLS) density (average CLS within 10 high-power fields, per animal) and mean adipocyte surface area (average surface area of 30 randomly sorted adipocytes, per animal) were determined using Imagelab Analysis software (version 2.4), as described previously (16).

Electron microscopy. Ultrastructural examination followed standard procedures, as described elsewhere (17), with a Zeiss EM10 transmission electron microscope (Carl Zeiss, Oberkochen, Germany).

Measurement of hepatic triglyceride content. Liver was homogenized and tissue triglyceride content was determined as described previously (18).

Isolation of the stroma vascular fraction and adipocyte fraction of adipose tissue. Epididymal fat pads were excised and isolation of the stroma vascular fraction and adipocyte fraction of adipose tissue was performed as described previously (19).

Real-time PCR. Total RNA was obtained from the adipocyte and stromal vascular fractions of WAT of the four groups of mice, according to methods published previously (8,20). Quantitative PCR was run to determine the expressions of TNF-α and IL-6 in each tissue fraction using primers supplied with the commercially available assays from Applied Biosystems (Mm00443258_m1 and Mm00446190_m1, respectively). The reference gene was GAPD (TaqMan, Applied Biosystems). Results are expressed as relative expression values, according to a method published previously (8).

Glucose uptake, glycogen synthesis, insulin signaling, and TLR-related signal transduction pathways in isolated soleus muscle. Soleus muscles from C3H/HeJ, C57BL/10ScNCr (TLR4$^{-/-}$), and their respective control mice were isolated and incubated in the presence of palmitate for 4 h, as described previously (21). In some experiments, soleus muscles from C3H/HeJ mice and their controls were incubated in the presence of stearic and lauric acids for 4 h. In the basal state and 30 min after insulin treatment, glucose uptake and glycogen synthesis were measured. To investigate insulin signaling in these experiments, soleus muscles from C3H/HeJ and C57BL/10ScNCr (TLR4$^{-/-}$) mice and their respective controls were incubated with insulin (10 mU/ml) for a further 5 min.

In some experiments, isolated soleus muscles from C3H/HeJ and C3H/HeN mice were incubated with LPS or palmitate for 1 h or preincubated in the absence (control group) or presence of 10 μg/ml of an antagonist monoclonal antibody to TLR4 (MTS510) (22) and then in the absence or presence of LPS for 1 h or palmitate for 4 h. At the end of the incubation period, muscles were homogenized and then centrifuged, as described previously (21). The supernatants were used for immunoprecipitation and immunoblotting.

Oxygen consumption and respiratory exchange ratio determination. Oxygen consumption and respiratory exchange ratio (RER) were measured in fed animals through an indirect open circuit calorimeter (Oxymax Deluxe System; Columbus Instruments, Columbus, OH), as described previously (23).

Tissue extraction, immunoprecipitation, and immunoblotting. Mice were anesthetized by intraperitoneal injection of sodium thiopental and used 10–15 min later, i.e., as soon as anesthesia was assured by the loss of pedal and corneal reflexes. Five minutes after the insulin injection (3.8 units/kg i.p.) muscle, adipose tissue, and liver were removed, minced coarsely, and homogenized immediately in extraction buffer, as described elsewhere (24). Extracts were then centrifuged at 15,000 rpm and 4°C for 40 min to remove insoluble material, and the supernatants were used for immunoprecipitation with α-insulin receptor (IR), IRS-1, and protein A-Sepharose 6MB (Pharmacia, Uppsala, Sweden). We performed immunoblotting on tissue extracts, as described previously (24).

Determination of NF-κB activation. NF-κB p50 activation was determined in nuclear extracts from muscle and adipose tissue by ELISA (89858; Pierce Biotechnology), according to the recommendations of the manufacturer.

Statistical analysis. Data are expressed as means ± SE, and the number of independent experiments is indicated. For statistical analysis, the groups were compared using a two-way ANOVA with the Bonferroni test for post hoc comparisons. The level of significance adopted was $P < 0.05$.

RESULTS

Body weight, food intake, epididymal fat pad, and leptin levels of C3H/HeJ and control mice. Six-week-old male mice with a loss-of-function (Pro^{712}His) mutation in TLR4 (C3H/HeJ) and a strain-specific control (C3H/HeN) were fed a HFD, and control groups of each genotype were fed a standard mouse chow diet. Body weight after 8 weeks of the HFD was lower for the C3H/HeJ mice than for the control mice (Fig. 1*A*). After 8 months of the HFD diet, this difference was more evident. Eight-month-old C3H/HeJ mice fed a HFD weighed on average 15% less than HFD-fed control mice (Fig. 1*B*). Daily food intake was similar in control and C3H/HeJ mice, fed either a HFD or standard chow (Fig. 1*C*); however, 8-week cumulative food intake was higher for the HFD in both genotypes (data not shown). The epididymal fat pad weights of control and C3H/HeJ mice fed a chow diet were similar; however, when groups fed a HFD were compared, the average weight of epididymal fat depots was decreased by 40% in the C3H/HeJ mice (Fig. 1*D*). In addition, consumption of a HFD led to a 36% lower increase in blood leptin levels in C3H/HeJ than in control mice (Fig. 1*E*).

Adipose tissue morphology and ultrastructural features of adipose tissue of C3H/HeJ and control mice fed a HFD. We assessed whether these differences in HFD-induced weight gain were related to alterations in adiposity. Morphometric analysis (Fig. 1*F–I*) revealed that adipocytes from C3H/HeJ mice fed a HFD were consistently smaller than adipocytes from control mice fed a HFD with an average 30% decrease in size (Fig. 1*J*). In addition, the frequency and distribution of mature macrophages in fixed WAT differed among the groups. As described previously (25), macrophages were aggregated in CLSs, which contained up to 15 macrophages surrounding what appeared to be individual adipocytes. CLS formation was a rare event in control mice (1.0 ± 0.5) (Fig. 1*F*) or in C3H/HeJ mice (1.0 ± 0.5) (Fig. 1*H*) but was increased >100-fold (105.5 ± 7.8) in control mice fed a HFD (Fig. 1*G*) and only ~10-fold (11.5 ± 2.1) in C3H/HeJ mice fed a HFD (Fig. 1*I*), indicating a much lower macrophage infiltration in WAT of the latter group. Ultrastructural analysis showed that CLSs were always composed of a dead adipocyte encircled by several typical macrophages. In control mice or C3H/HeJ mice fed a HFD, adipocyte death exhibited none of the classical features of apoptosis. Instead, in both groups, features consistent with necrosis (such as disruption of basal membranes, intracytoplasmic organelle degeneration, and cell debris) were commonly found, but necrosis was more evident in control mice fed a HFD (data not shown).

Increased metabolic rates in C3H/HeJ mice fed a HFD. We examined whether the decreased body weight in C3H/HeJ mice fed a HFD resulted from increased energy expenditure. The oxygen consumption rates of control and C3H/HeJ mice fed normal chow were similar (Fig. 2*A*). However, after 8 weeks of a HFD, C3H/HeJ mice exhibited significantly higher rates of O_2 consumption than control mice (Fig. 2*A*). The RERs of control and C3H/HeJ mice fed a chow diet were similar (Fig. 2*B*). In contrast, the RER was lower in C3H/HeJ mice fed a HFD than in control mice (Fig. 2*B*), indicating that these animals were largely using fatty acids as an energy source.

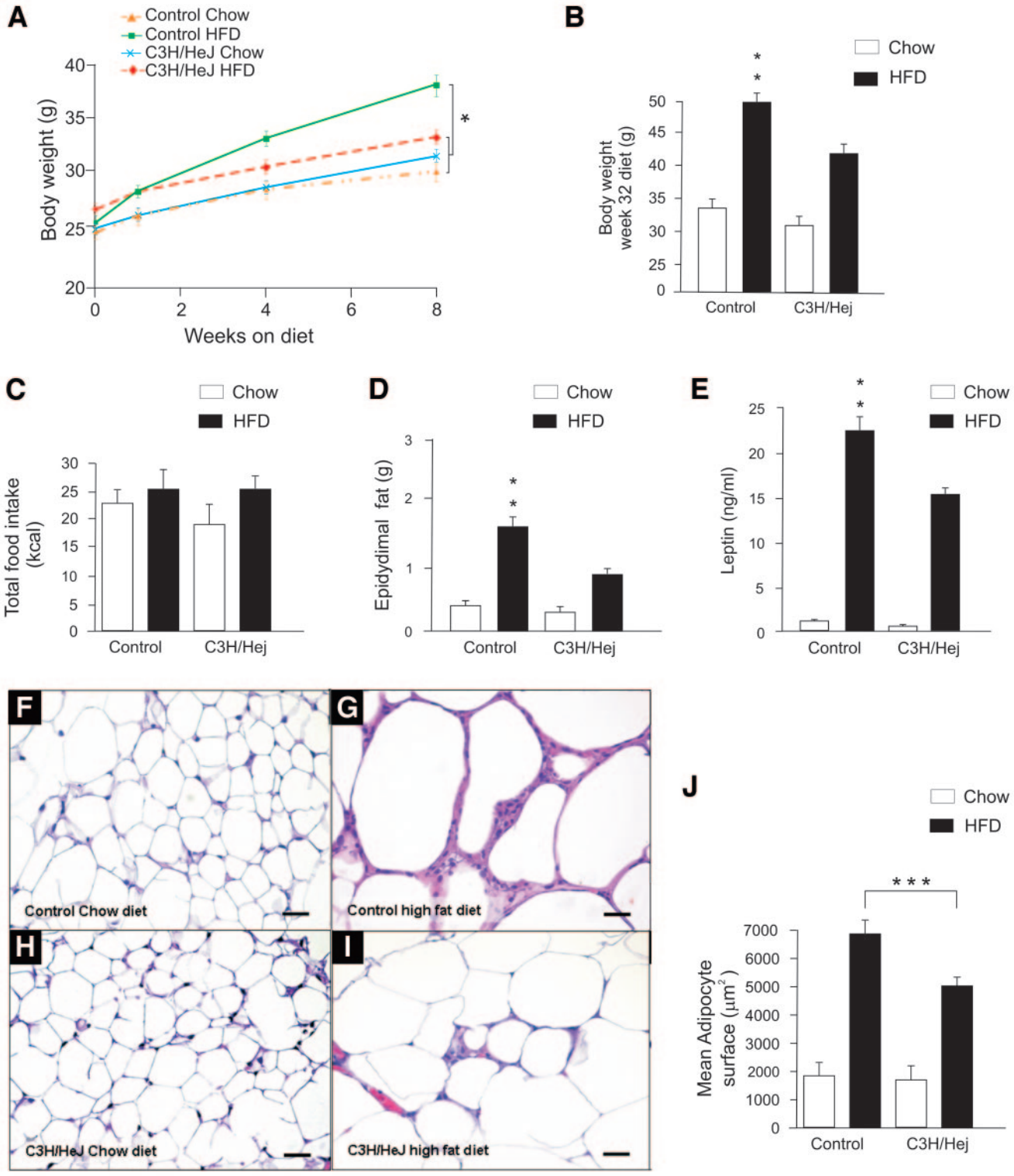

FIG. 1. Protection against diet-induced obesity in C3H/HeJ and adipose tissue morphology in control and C3H/HeJ mice. *A*: Body weight of C3H/HeJ and control mice fed a HFD and chow diet. *B*: Body weight of 8-month-old control and C3H/HeJ mice. *C*: Daily food intake with regular chow and a HFD. *D*: Epididymal fat pad weights. *E*: Week 8 fasting leptin concentrations. *F–I*: Histological sections of epididymal fat pads from control mice (*F*) and C3H/HeJ mice (*H*) fed on a chow diet and control mice (*G*) and C3H/HeJ mice (*I*) fed a HFD diet; 50-μm scale bar for all pictures. *J*: Mean adipocyte surface (square micrometers). Data are means ± SE from six to eight mice per group. **P* < 0.05 (control mice fed a HFD versus all others groups); ***P* < 0.01 (control mice fed a HFD versus all others groups); ****P* < 0.01 between groups, as indicated.

Serum FFA, TNF-α, IL-6, adiponectin, and hepatic triglyceride content in C3H/HeJ mice and control mice fed a HFD. We examined serum concentrations of adiponectin, IL-6, TNF-α, and FFAs, which have postulated roles in obesity and insulin action (26–34). Adiponectin levels were comparable between control and C3H/HeJ mice fed a chow diet (Fig. 2*C*). In contrast, adiponectin levels were reduced in control mice fed a HFD, but not in C3H/HeJ mice fed the same diet (control + HFD 7.1 ± 0.4 vs. C3H/HeJ + HFD 9.5 ± 0.6 μg/ml, $P < 0.001$) (Fig. 2*C*).

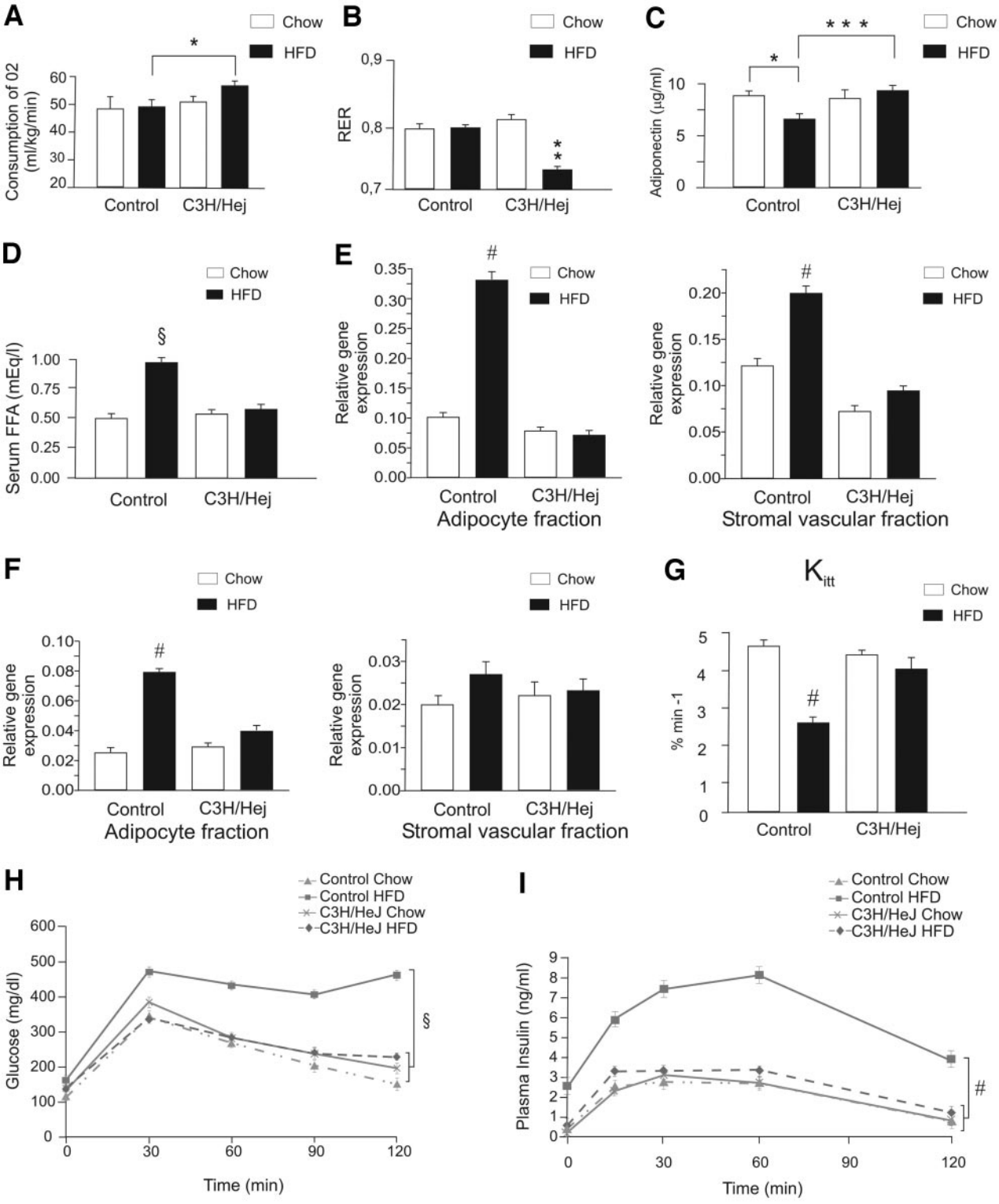

FIG. 2. Metabolic parameters, adipokines, insulin, and glucose tolerance in control and C3H/HeJ mice fed a chow or a HFD diet. *A*: Oxygen consumption. *B*: RER. *C*: Week 8 fasting adiponectin concentrations. *D*: Fasting FFA concentrations. *E*: Determination of the relative TNF-α mRNA expression by real-time PCR. *F*: Determination of the relative IL-6 mRNA expression by real-time PCR. *G*: Insulin tolerance test after 8 weeks of the diet. *H*: Glucose tolerance test after 8 weeks of the diet. *I*: Insulin response curve during the glucose tolerance test after 8 weeks of the diet. **P* < 0.05 between groups, as indicated; ***P* < 0.001 (C3H/HeJ mice fed a HFD versus all other groups); ****P* < 0.001 (control mice fed a HFD versus C3H/HeJ mice fed a HFD); #*P* < 0.05 (control mice fed a HFD versus all other groups); §*P* < 0.01 (control mice fed a HFD versus all other groups). Data are means ± SE from six to eight mice.

An analysis of FFAs showed no difference between control and C3H/HeJ mice fed the chow diet (Fig. 2*D*). In contrast, the increase in FFA levels observed in mice fed a HFD was less pronounced in C3H/HeJ mice than in control mice (Fig. 2*D*). Serum TNF-α and IL-6 levels were only detectable in mice fed a HFD, and these levels were higher in the

control mice than in C3H/HeJ mice (TNF-α: control + HFD 467.71 ± 87.8 vs. C3H/HeJ + HFD 115.2 ± 73.11, $P < 0.001$; IL-6: control + HFD 249.43 ± 55.12 vs. C3H/HeJ + HFD 47.54 ± 42.25, $P < 0.001$). The relative amount of TNF-α transcript was significantly increased in the adipocyte and stromal vascular fractions of control mice fed a HFD compared with control and C3H/HeJ mice fed a chow diet and C3H/HeJ mice fed a HFD (Fig. 2*E*). A significant increase of IL-6 expression was detected in the adipocyte but not stromal vascular fraction of control mice fed a HFD. This effect was absent in C3H/HeJ mice fed a HFD (Fig. 2*F*). We next measured hepatic triglyceride content and found similar values between control and C3H/HeJ mice fed a chow diet. However, with the HFD, hepatic triglyceride increased more in the control than in the C3H/HeJ livers (35 ± 7.5 vs. 22 ± 6.2 mg/g, $P < 0.05$).

Improved glucose tolerance and insulin tolerance in C3H/HeJ mice. To investigate insulin and glucose tolerance, we performed an insulin tolerance test and an intraperitoneal glucose tolerance test (IGTT) and determined serum insulin levels at some time points during the IGTT. The glucose disappearance rate in response to insulin was lower in control than in C3H/HeJ mice fed a HFD (Fig. 2*G*). This rate was indistinguishable between control and C3H/HeJ mice fed a chow diet (Fig. 2*G*). During the IGTT, after glucose infusion, the blood glucose levels of HFD-fed control mice were greater at all time points. In contrast, C3H/HeJ mice fed a HFD were protected against the development of glucose intolerance (Fig. 2*H*), as previously described (35). In addition, serum insulin levels at all time points during the IGTT in C3H/HeJ mice fed a HFD were significantly lower than those in control mice fed the same diet (Fig. 2*I*).

Insulin signaling in muscle and WAT of C3H/HeJ and control mice fed a HFD. In muscle, insulin-induced IRβ, IRS-1 tyrosine phosphorylation, and Akt phosphorylation were reduced by 50–70% in control mice fed a HFD compared with C3H/Hej mice fed the same diet (Fig. 3*A–C*), and these reductions were accompanied by a 50% reduction in IRS-1 protein content in the skeletal muscle (Fig. 3*B*). In WAT, insulin-mediated IRβ, IRS-1 tyrosine phosphorylation, and Akt phosphorylation were reduced by 50–70% in control mice fed a HFD (Fig. 3*D–F*), and there was a 70% reduction in IRS-1 protein concentration (Fig. 3*E*). In contrast, high-fat feeding did not impair the stimulatory effect of insulin on IRβ, IRS-1, and Akt phosphorylation in WAT of C3H/Hej mice fed on a HFD (Fig. 3*D–F*).

Ser^{307} Phosphorylation of IRS-1 and activation of JNK and IKKβ in muscle and WAT of high-fat–fed C3H/HeJ and control mice. We tested Ser^{307} phosphorylation of IRS-1 in muscle and WAT of control and C3H/HeJ mice. Ser^{307} phosphorylation was induced by a HFD in both tissues of control mice but not in tissues of C3H/HeJ mice (Fig. 4*A*). IKKβ activity was monitored using IκBα protein abundance as described previously (36). IκBα protein levels were reduced in muscle and adipose tissue of control but not C3H/HeJ mice fed a HFD (Fig. 4*B*). We also measured NF-κB nuclear subunit p50 activation and found an increase in the DNA binding of nuclear p50 in muscle and adipocytes of control mice fed a HFD but not in the other groups (Fig. 4*C*). JNK activation was determined by monitoring phosphorylation of JNK (Thr^{183} and Tyr^{185}) and c-Jun (Ser^{63}), which is a substrate of JNK. In a similar fashion, JNK phosphorylation was increased in adipose tissue and muscle of control but not C3H/HeJ mice fed a HFD (Fig. 4*D*).

Insulin signaling and activation of JNK and IKKβ in the liver of high-fat–fed C3H/HeJ and control mice. We next investigated insulin signaling in the livers of C3H/HeJ and control mice. We detected a 50% reduction in insulin-induced IRS-1 tyrosine phosphorylation accompanied by a 30% reduction in IRS-1 protein content (Fig. 5*A*) and a 70% reduction in Akt phosphorylation (Fig. 5*B*) in the livers of control mice fed a HFD but not in C3H/HeJ mice fed the same diet. Ser^{307} phosphorylation of IRS-1 and JNK phosphorylation were increased and IκBα protein expression was decreased in the livers of control but not C3H/HeJ mice fed a HFD (Fig. 5*C–E*).

Protection from palmitate, stearic, and lauric acid–induced insulin resistance in isolated soleus muscle of C3H/HeJ and TLR4 knockout mice. It has recently been reported that TLR4 is activated by FFAs (37). We examined glucose uptake and glycogen synthesis in the presence of 100 μmol/l palmitate for 4 h. Palmitate treatment reduced insulin-stimulated glucose uptake and glycogen synthesis by 40–50% in isolated soleus muscle from control mice but not in isolated soleus muscle from C3H/HeJ mice (Fig. 6*A* and *B*). In accordance with this finding, palmitate induced a downregulation in insulin-induced IR (40%), IRS-1 (50%), and Akt (60%) phosphorylation in isolated soleus muscle of control mice but not in muscle of C3H/HeJ mice (Fig. 6*C–E*). We also investigated the effect of lauric and stearic acid on glucose metabolism and insulin signaling in isolated muscle. Stearic and lauric acid treatments reduced glucose uptake by ~40% and only 20%, respectively, in isolated soleus muscle from control mice but not in isolated soleus muscle from C3H/HeJ mice (Fig. 6*F*). We next investigated insulin signaling in isolated soleus muscle from control and C3H/HeJ mice after stearic and lauric acid treatments. We observed a downregulation in insulin-induced IR and IRS-1 tyrosine phosphorylation (data not shown) and Akt phosphorylation (reductions of 41 ± 4 and 63 ± 7%, respectively, for lauric and stearic acids) in isolated soleus muscle of control mice but not in the muscle of C3H/HeJ mice (Fig. 6*G*). Furthermore, we repeated the same protocol in isolated soleus muscle from TLR4$^{-/-}$ and the respective control mice, and a protection from palmitate-induced insulin resistance related to glucose uptake, glycogen synthesis, and insulin signaling (data not shown) was also observed in isolated muscle from TLR4$^{-/-}$ mice.

Palmitate treatment activates TLR4 signal transduction in isolated soleus muscle of control mice. We next examined the effect of palmitate treatment on TLR4 activation compared with that of a known TLR4 agonist, LPS. Similarly to LPS, palmitate administration induced the association of TLR4 with the adaptor protein, MyD88, in isolated muscle from control mice but not in muscle from C3H/HeJ mice (Fig. 7*A* and *B*). Palmitate treatment induced degradation of IκBα and increased JNK phosphorylation and IRS-1 Ser^{307} phosphorylation in isolated muscle from control mice but not in isolated muscle from C3H/HeJ mice (Fig. 7*C–E*). We measured the NF-κB nuclear subunit p50 activation after palmitate treatment and found an increase in the DNA binding of nuclear p50 in isolated muscle of control mice but not in muscle from C3H/HeJ mice (Fig. 7*F*).

Treatment of isolated soleus muscle of control mice with a TLR4 antagonistic antibody blocks palmitate-

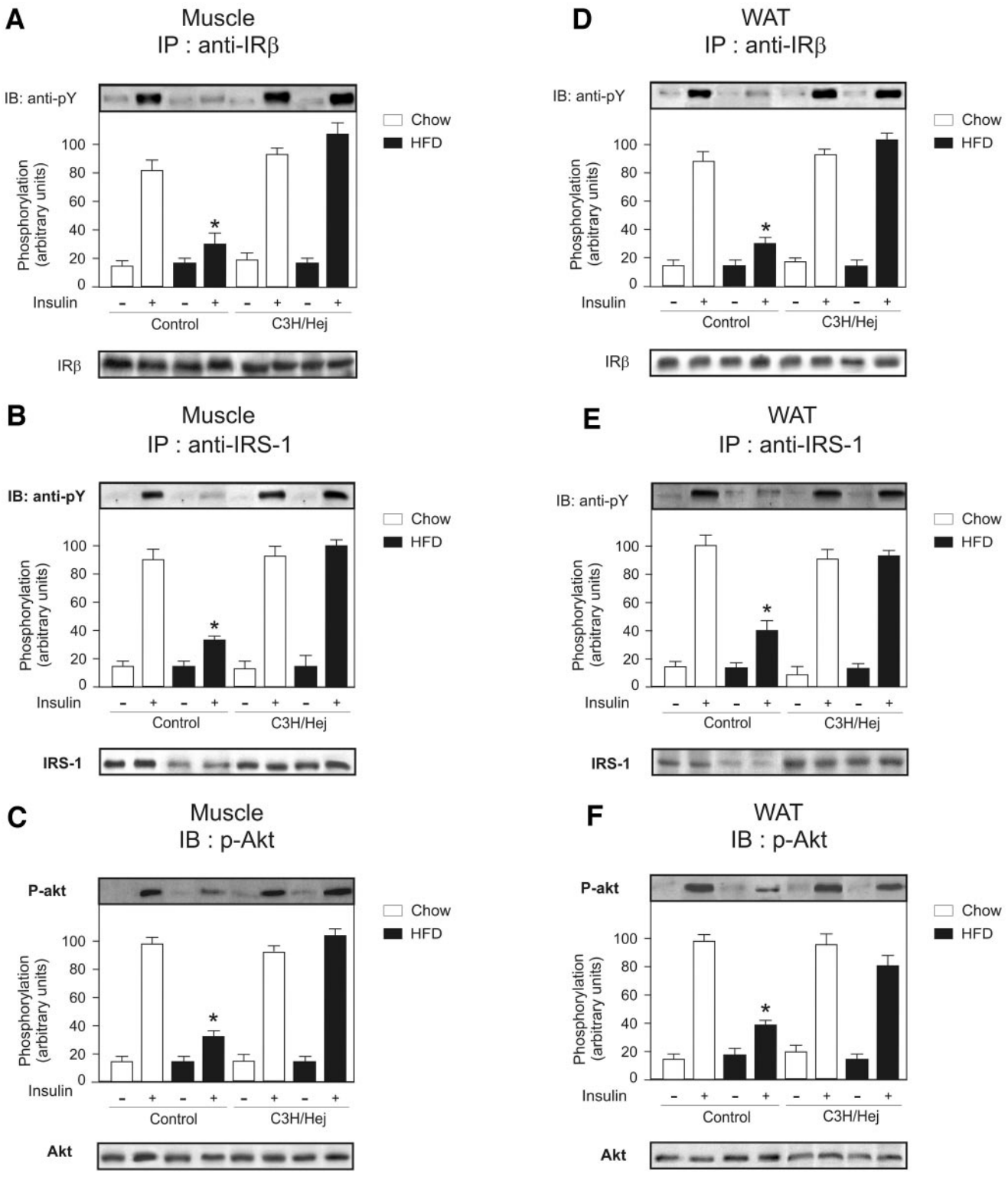

FIG. 3. Effects of high-fat feeding on insulin-signaling components in muscle and WAT of control and C3H/HeJ mice fed a 2-month diet. *A* and *D*: Insulin-induced tyrosine phosphorylation of IR. *B* and *E*: Insulin-induced tyrosine phosphorylation of IRS-1 and IRS-1 protein level. *C* and *F*: Insulin-induced serine phosphorylation of Akt. Bars represent means ± SE from six to eight mice. *$P < 0.05$ (insulin-stimulated control mice fed a HFD versus all others groups also stimulated with insulin). IB, immunoblot; IP, immunoprecipitate.

induced insulin resistance. To reinforce the importance of TLR4 in the development of insulin resistance, we investigated whether the inhibition of TLR4, through the use of the TLR4 antagonist antibody MTS510, could reverse LPS- and palmitate-induced inhibition of insulin-induced IR/IRS-1 and Akt phosphorylation. Isolated soleus muscles of control mice were pretreated with MTS510 for 1 h before exposure to 100 μmol/l palmitate. The results showed that MTS510 treatment prevented palmitate-induced reduced insulin-stimulated glucose uptake (Fig. 8*A*) and glycogen synthesis (data not shown). In addition, we found that MTS510 treatment prevented the deleteri-

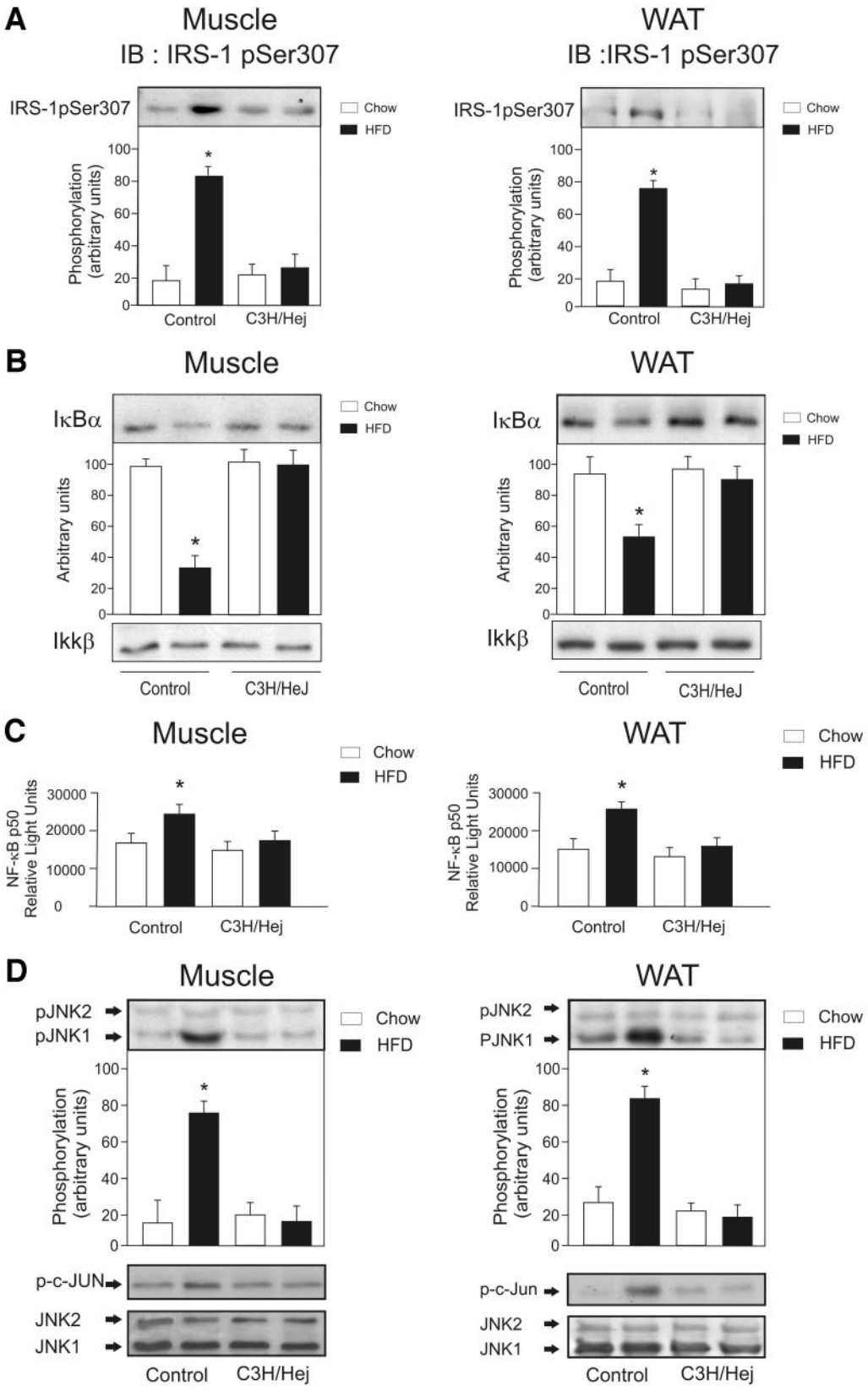

FIG. 4. Effects of high-fat feeding on Ser^{307} phosphorylation of IRS1 and reduced IKKβ activity and JNK activation in muscle and WAT of C3H/HeJ mice fed a HFD compared with control mice. *A*: Ser^{307} phosphorylation of IRS1 in muscle and WAT. *B*: IκBα protein levels. *C*: Transcription factor binding assay of NF-κB p50 nuclear extracts from muscle and WAT. *D*: Phosphorylation of JNK and Jun. Representative blots are shown from experiments that were repeated independently at least three times with similar results. *$P < 0.05$ (control mice fed a HFD versus all others groups).

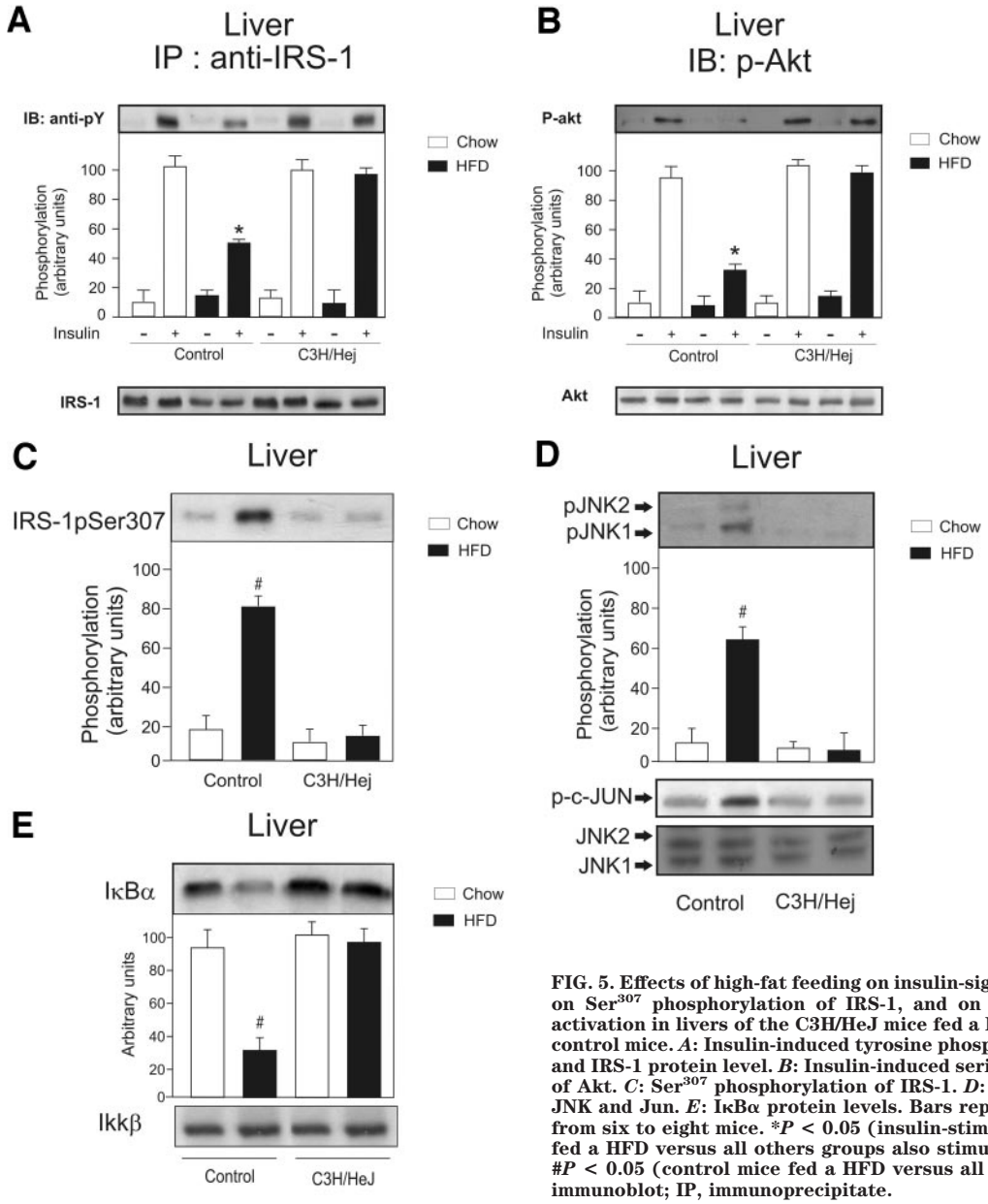

FIG. 5. Effects of high-fat feeding on insulin-signaling components, on Ser^{307} phosphorylation of IRS-1, and on JNK and on IKKβ activation in livers of the C3H/HeJ mice fed a HFD compared with control mice. *A*: Insulin-induced tyrosine phosphorylation of IRS-1 and IRS-1 protein level. *B*: Insulin-induced serine phosphorylation of Akt. *C*: Ser^{307} phosphorylation of IRS-1. *D*: Phosphorylation of JNK and Jun. *E*: IκBα protein levels. Bars represent means ± SE from six to eight mice. **P* < 0.05 (insulin-stimulated control mice fed a HFD versus all others groups also stimulated with insulin); #*P* < 0.05 (control mice fed a HFD versus all others groups). IB, immunoblot; IP, immunoprecipitate.

ous effects of LPS and palmitate on insulin signaling (Fig. 8*B–D*). Furthermore, isolated muscle preincubated with MTS510 antibody demonstrated a significant decrease in palmitate-induced IκBα degradation and JNK phosphorylation (Fig. 8*E* and *F*).

DISCUSSION

Here we show that C3H/HeJ mice, which have a loss-of-function mutation in TLR4, are protected against the development of diet-induced obesity and insulin resistance. In addition, in isolated muscles from C3H/HeJ mice, there was a protection from saturated fatty acid–induced insulin resistance.

The C3H/HeJ mice fed a HFD gain less weight without changing food intake, have a reduced adipose mass, and demonstrate a less pronounced increase in adipocyte size than their controls. Recently, Shi et al. (38) showed that female but not male TLR4$^{-/-}$ mice fed a HFD had increased body weight, associated with increased food intake, compared with control mice. The reason for the difference in body weight and food intake between female TLR4$^{-/-}$ mice fed a HFD and HFD-fed C3H/HeJ mice, which have an inactivation mutation in TLR4 is not clear but may be related, at least in part, to sex, strain, and the type of genetic alteration in TLR4. In this regard, some responses may be different in animals with point mutations or in knockout animals, as described previously (39,40), and we may hypothesize that C3H/HeJ or TLR4$^{-/-}$ mice may not have exactly the same regulation of food intake and/or energy expenditure; however, this point deserves further investigation.

The protection from diet-induced obesity in C3H/HeJ mice fed a HFD is linked to an increase in oxygen consumption and a decrease in RER, indicating that these animals were largely using fatty acids as an energy source. Taken together, these results demonstrate that the attenuation of diet-induced weight gain in C3H/HeJ mice is associated with a decreased adipocyte size, decreased macrophage infiltration in WAT, and increased energy expenditure and fat oxidation in the context of dietary

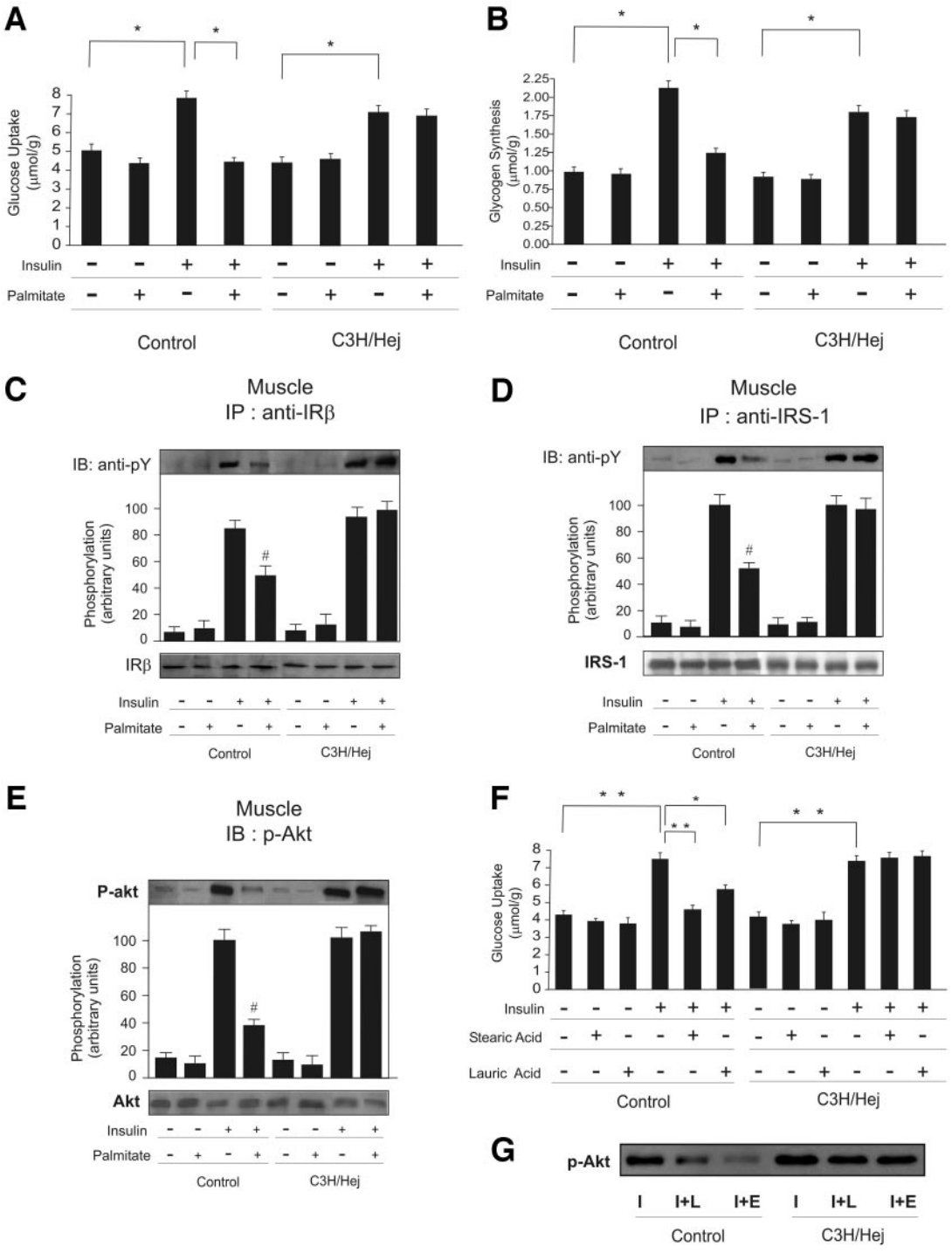

FIG. 6. Protection from saturated fatty acid–induced insulin resistance in isolated muscle of C3H/HeJ mice. *A*: Effect of palmitate on insulin-induced glucose uptake in isolated soleus muscle from control and C3H/HeJ mice. *B*: Effect of palmitate on insulin-induced glycogen synthesis in soleus muscles from control and C3H/HeJ mice. *C–E*: Effect of palmitate on insulin-stimulated phosphorylation of IR (*C*), IRS-1 (*D*), and Akt (*E*) in C3H/HeJ and control mice. *F*: Effect of stearic and lauric acids on insulin-induced glucose uptake in isolated soleus muscle from control and C3H/HeJ mice. *G*: Effect of stearic and lauric acids on insulin-stimulated phosphorylation of Akt. *$P < 0.05$ between groups, as indicated; **$P < 0.01$ between groups, as indicated; #$P < 0.05$ (insulin + palmitate versus insulin alone in control mice). Representative blots are shown from experiments that were repeated independently at least three times with similar results. I, insulin; I+E, insulin + stearic acid; I+L, insulin + lauric acid; IB, immunoblot; IP, immunoprecipitate.

obesity. In addition, the attenuated increase in FFAs, TNF-α, and IL-6 in C3H/HeJ mice fed a HFD was associated with protection from glucose intolerance and insulin resistance. During the preparation of this article, Suganami et al. (41) and Poggi et al. (42) also reported that C3H/HeJ mice have attenuated adipose tissue inflammation compared with control mice during feeding of a HFD.

The blunted insulin-stimulated IR tyrosine phosphorylation and phosphorylation of Akt in muscle, WAT, and liver of HFD-fed control mice was prevented in C3H/HeJ mice, providing a biochemical correlate for increased in vivo insulin sensitivity. Serine phosphorylation of IRS-1 has been proposed as a general mechanism of functional inhibition of the IRS-1 protein, and Ser^{307} phosphorylation

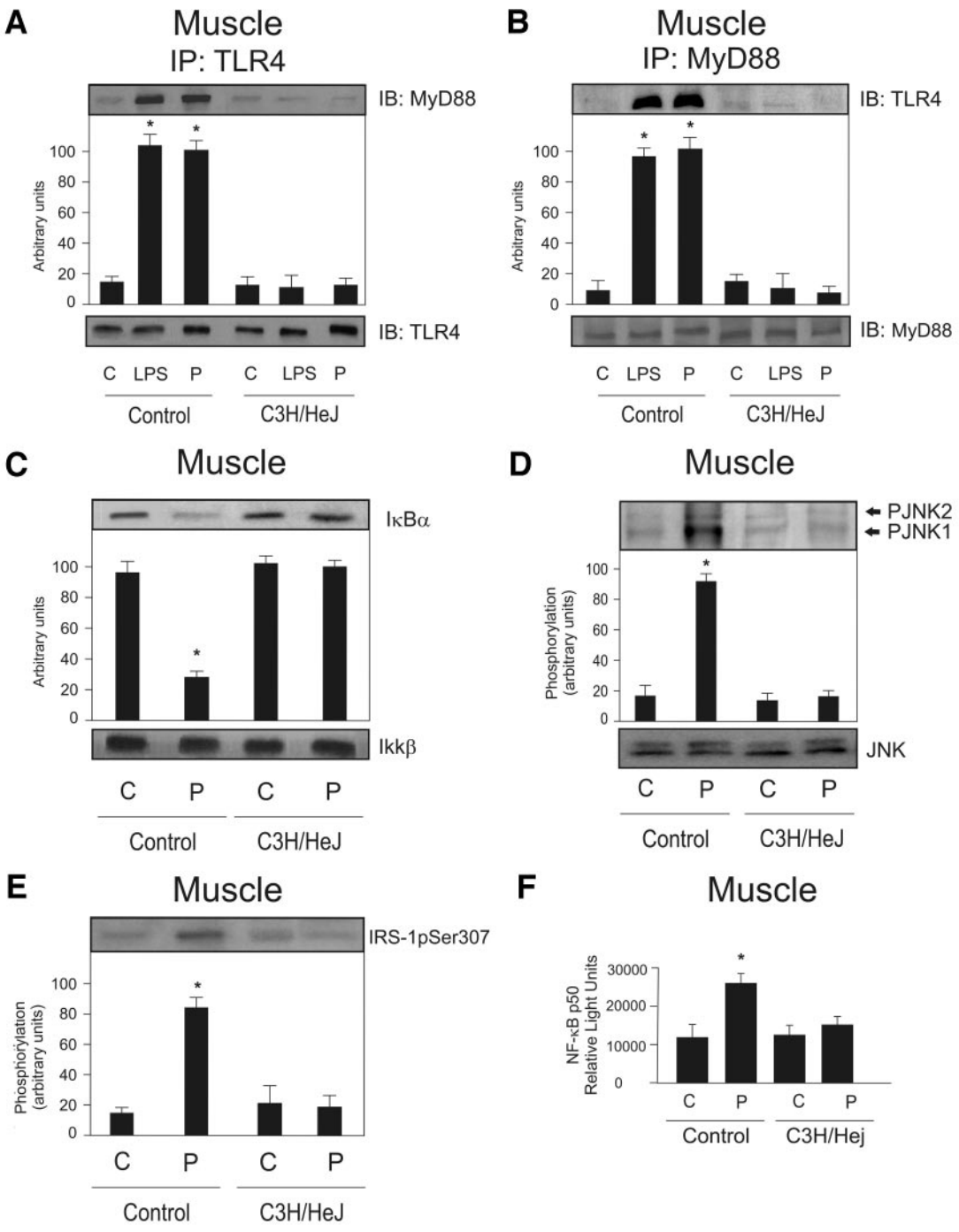

FIG. 7. Protection from palmitate activation of TLR-related signal transduction pathways in isolated muscle of C3H/HeJ mice. Coimmunoprecipitation of MyD88 with TLR4 receptor (*A*) and of TLR4 with MyD88 (*B*) in isolated muscles from C3H/Hej and control mice. *C*: IκBα protein levels. *D*: phosphorylation of JNK. *E*: Ser^{307} phosphorylation of IRS1. *F*: Transcription factor binding assay of NF-κB p50 nuclear extracts from isolated soleus muscle. **P* < 0.05 (LPS or palmitate versus basal control in control mice). C, control; IB, immunoblot; IP, immunoprecipitate; P, palmitate. Representative blots are shown from experiments that were repeated independently at least three times with similar results.

has become a molecular indicator of insulin resistance (3,4,43,44). Ser^{307} phosphorylation was induced by the HFD in tissues of HFD-fed control mice, accompanied by a reduction in IRS-1 protein expression in muscle, WAT, and liver and in insulin-induced IRS-1 tyrosine phosphorylation levels. This regulation of IRS-1, induced by the HFD, was prevented in C3/HeJ mice.

Ser^{307} is reported to be a phosphoacceptor of JNK and IKKβ (43,44), and, as described previously (1,3), our results also show that these kinases are activated in tissues of HFD-fed control mice. It is well known that the activation of TLR4 induces a complex signaling pathway that activates IKKβ and JNK (10). Our data demonstrating that a point mutation in TLR4, which inactivates this receptor, prevents diet-induced obesity, activation of IKKβ and JNK, and insulin resistance suggest that TLR4 is a key modulator in the cross-talk between inflammatory and metabolic pathways.

Despite the protection from diet-induced insulin resistance related to a reduction in adipose mass, a direct effect

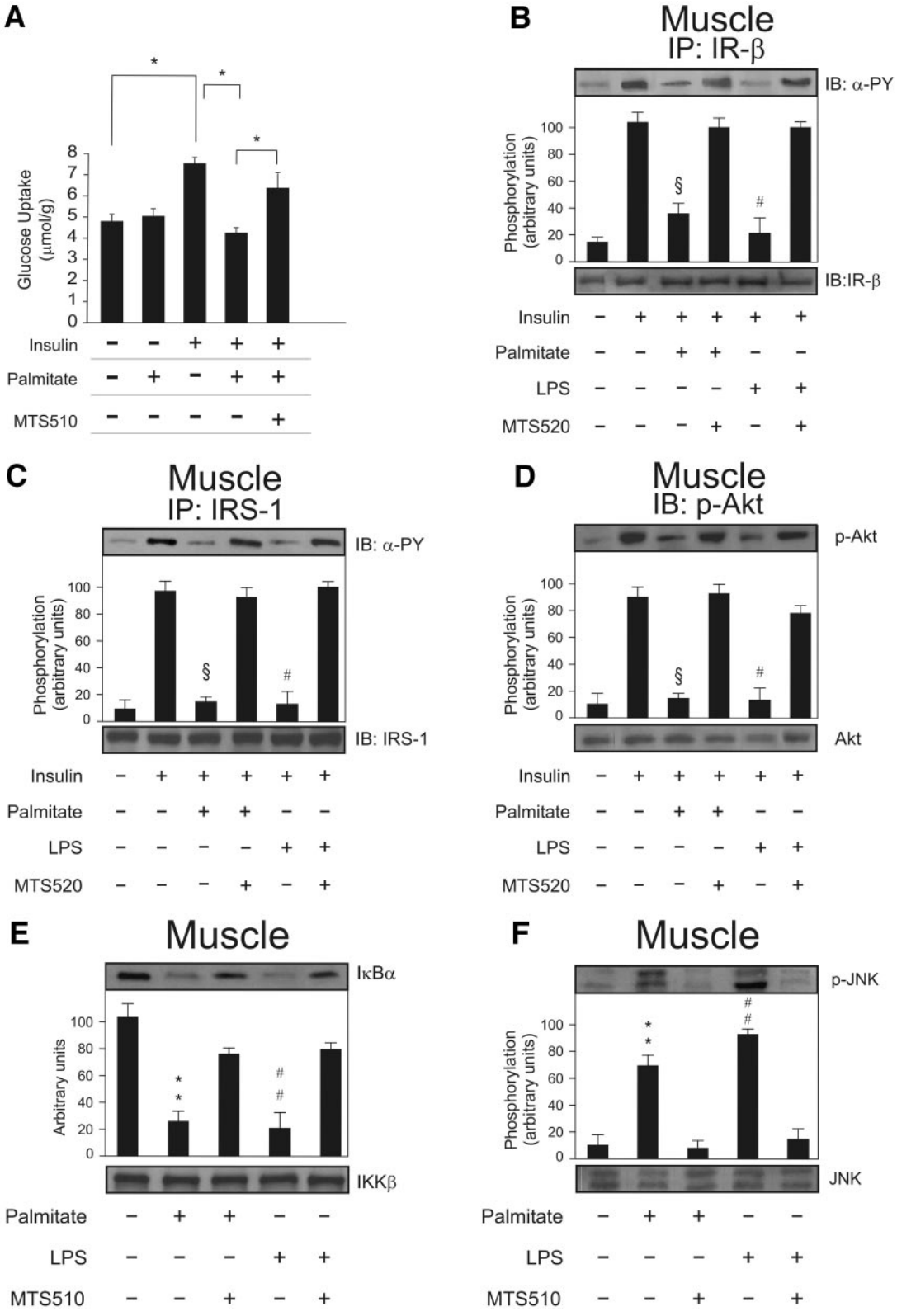

FIG. 8. The antagonist monoclonal TLR4 antibody (MTS510) inhibits palmitate-induced insulin resistance and activation of TLR4-related signal transduction pathways. *A*: Effect of palmitate on insulin-induced glucose uptake in isolated soleus muscle from control mice pretreated with MTS510. Effect of palmitate on insulin-induced phosphorylation of the IR (*B*), IRS-1 (*C*), and Akt (*D*) in isolated soleus muscle from control mice pretreated with MTS510. *E*: IκBα protein levels. *F*: Phosphorylation of JNK. **P* < 0.05 between groups, as indicated; §*P* < 0.05 (insulin + palmitate versus insulin alone); #*P* < 0.05 (insulin + LPS versus insulin alone); ***P* < 0.05 (palmitate versus basal control); ##*P* < 0.05 (LPS versus basal control). Representative blots are shown from experiments that were repeated independently at least three times with similar results. IB, immunoblot; IP, immunoprecipitate.

of the TLR4 mutation on muscle tissue is also observed. Our data demonstrate that, in isolated muscle from control mice, palmitate induced the association of MyD88 with the TLR4 receptor, activated downstream kinases such as IKKβ and JNK, weakened insulin signal transduction, and reduced glucose uptake and glycogen synthesis; however, this effect was not observed in isolated muscle from C3H/HeJ and $TLR4^{-/-}$ mice. These data indicate that, independently of the changes in adipose tissue and in circulating FFAs, a loss of TLR4 function protects muscle from palmitate, stearic, and lauric acid–induced insulin resistance. In accordance with this finding, recent reports indicated that TLR2 or TLR4 is important for FFA-induced insulin resistance in myotubes or in adipocytes (38,45–47). In addition, it has been recently demonstrated by Shi et al. (38) that FFAs can act through TLR4 on adipose cells and macrophages to induce inflammatory signaling and suppress insulin signaling. Our data clearly show that palmitate and stearic acid, and to a lesser extent lauric acid, activate TLR4 signaling in muscle and that the capacity of these fatty acids to induce inflammatory signaling and to reduce insulin signaling and insulin-mediated glucose metabolism is blunted in muscle with a loss-of-function or absence of TLR4.

Our results also show that a known TLR4 ligand, LPS, is able to activate a pathway similar to those activated by palmitate treatment, inhibiting insulin signal transduction. In addition, the inhibition of TLR4, through the use of the TLR4 antagonist antibody, MTS510, could reverse LPS- and palmitate-induced inhibition of insulin-induced IR/IRS-1 and Akt phosphorylation. These data indicate that TLR4 activation by multiple factors may play an important role in the development of insulin resistance in sepsis and obesity and that the modulation of this receptor may prevent insulin resistance.

In summary, our data showing that a loss-of-function point mutation in TLR4 prevents diet-induced obesity, activation of IKKβ, JNK, and insulin resistance in mice fed a HFD, and also saturated fatty acid–induced insulin resistance in isolated muscle, indicate that TLR4 is a key modulator in the cross-talk between inflammatory and metabolic pathways. We, therefore, suggest that a selective interference with TLR4 presents an attractive opportunity for the treatment of human obesity, insulin resistance, and type 2 diabetes.

REFERENCES

1. Yuan M, Konstantopoulos N, Lee J, Hansen L, Li ZW, Karin M, Shoelson SE: Reversal of obesity- and diet-induced insulin resistance with salicylates or targeted disruption of Ikkβ. *Science* 293:1673–1677, 2001
2. Perreault M, Marette A: Targeted disruption of inducible nitric oxide synthase protects against obesity-linked insulin resistance in muscle. *Nat Med* 7:1138–1143, 2001
3. Hirosumi J, Tuncman G, Chang L, Gorgun CZ, Uysal KT, Maeda K, Karin M, Hotamisligil GS: A central role for JNK in obesity and insulin resistance. *Nature* 420:333–336, 2002
4. Lee YH, Giraud J, Davis RJ, White MF: c-Jun N-terminal kinase (JNK) mediates feedback inhibition of the insulin signaling cascade. *J Biol Chem* 278:2896–2902, 2003
5. Aguirre V, Uchida T, Yenush L, Davis R, White MF: The c-Jun NH_2-terminal kinase promotes insulin resistance during association with insulin receptor substrate-1 and phosphorylation of Ser^{307}. *J Biol Chem* 275:9047–9054, 2000
6. Arkan MC, Hevener AL, Greten FR, Maeda S, Li ZW, Long JM, Wynshaw-Boris A, Poli G, Olefsky J, Karin M: IKK-β links inflammation to obesity-induced insulin resistance. *Nat Med* 11:191–198, 2005
7. Cai D, Yuan M, Frantz DF, Melendez PA, Hansen L, Lee J, Shoelson SE: Local and systemic insulin resistance resulting from hepatic activation of IKK-β and NF-κB. *Nat Med* 11:183–190, 2005
8. Weisberg SP, McCann D, Desai M, Rosenbaum M, Leibel RL, Ferrante AW Jr: Obesity is associated with macrophage accumulation in adipose tissue. *J Clin Invest* 112:1796–1808, 2003
9. Xu H, Barnes GT, Yang Q, Tan G, Yang D, Chou CJ, Sole J, Nichols A, Ross JS, Tartaglia LA, Chen H: Chronic inflammation in fat plays a crucial role in the development of obesity-related insulin resistance. *J Clin Invest* 112:1821–1830, 2003
10. Takeda K, Kaisho T, Akira S: Toll-like receptors. *Annu Rev Immunol* 21:335–376, 2003
11. Beutler B: Inferences, questions and possibilities in Toll-like receptor signalling. *Nature* 430:257–263, 2004
12. Akira S, Uematsu S, Takeuchi O: Pathogen recognition and innate immunity. *Cell* 124:783–801, 2006
13. Poltorak A, He X, Smirnova I, Liu MY, Van Huffel C, Du X, Birdwell D, Alejos E, Silva M, Galanos C, Freudenberg M, Ricciardi-Castagnoli P, Layton B, Beutler B: Defective LPS signaling in C3H/HeJ and C57BL/10ScCr mice: mutations in Tlr4 gene. *Science* 282:2085–2088, 1998
14. Lee JY, Ye J, Gao Z, Youn HS, Lee WH, Zhao L, Sizemore N, Hwang DH: Reciprocal modulation of Toll-like receptor-4 signaling pathways involving MyD88 and phosphatidylinositol 3-kinase/AKT by saturated and polyunsaturated fatty acids. *J Biol Chem* 278:37041–37051, 2003
15. Carvalho-Filho MA, Ueno M, Hirabara SM, Seabra AB, Carvalheira JB, de Oliveira MG, Velloso LA, Curi R, Saad MJ: S-Nitrosation of the insulin receptor, insulin receptor substrate 1, and protein kinase B/Akt: a novel mechanism of insulin resistance. *Diabetes* 54:959–967, 2005
16. Schenka AA, Machado CM, Grippo MC, Queiroz LS, Schenka NG, Chagas CA, Verinaud L, Brousset P, Vassallo J: Immunophenotypic and ultrastructural validation of a new human glioblastoma cell line. *Cell Mol Neurobiol* 25:929–941, 2005
17. Metze K, Andrade LA: Atypical stromal giant cells of cervix uteri—evidence of Schwann cell origin. *Pathol Res Pract* 187:1031–1035; discussion 1036–1038, 1991
18. Kanda H, Tateya S, Tamori Y, Kotani K, Hiasa K, Kitazawa R, Kitazawa S, Miyachi H, Maeda S, Egashira K, Kasuga M: MCP-1 contributes to macrophage infiltration into adipose tissue, insulin resistance, and hepatic steatosis in obesity. *J Clin Invest* 116:1494–1505, 2006
19. Lumeng CN, Bodzin JL, Saltiel AR: Obesity induces a phenotypic switch in adipose tissue macrophage polarization. *J Clin Invest* 117:175–184, 2007
20. Bertelli DF, Araujo EP, Cesquini M, Stoppa GR, Gasparotto-Contessotto M, Toyama MH, Felix JV, Carvalheira JB, Michelini LC, Chiavegatto S, Boschero AC, Saad MJ, Lopes-Cendes I, Velloso LA: Phosphoinositide-specific inositol polyphosphate 5-phosphatase IV inhibits inositide trisphosphate accumulation in hypothalamus and regulates food intake and body weight. *Endocrinology* 147:5385–5399, 2006
21. Massao Hirabara S, de Oliveira Carvalho CR, Mendonca JR, Piltcher Haber E, Fernandes LC, Curi R: Palmitate acutely raises glycogen synthesis in rat soleus muscle by a mechanism that requires its metabolization (Randle cycle). *FEBS Lett* 541:109–114, 2003
22. Akashi S, Shimazu R, Ogata H, Nagai Y, Takeda K, Kimoto M, Miyake K: Cutting edge: Cell surface expression and lipopolysaccharide signaling via the toll-like receptor 4-MD-2 complex on mouse peritoneal macrophages. *J Immunol* 164:3471–3475, 2000
23. Hirabara SM, Silveira LR, Alberici LC, Leandro CV, Lambertucci RH, Polimeno GC, Cury Boaventura MF, Procopio J, Vercesi AE, Curi R: Acute effect of fatty acids on metabolism and mitochondrial coupling in skeletal muscle. *Biochim Biophys Acta* 1757:57–66, 2006
24. Thirone AC, Carvalheira JB, Hirata AE, Velloso LA, Saad MJ: Regulation of Cbl-associated protein/Cbl pathway in muscle and adipose tissues of two animal models of insulin resistance. *Endocrinology* 145:281–293, 2004
25. Cinti S, Mitchell G, Barbatelli G, Murano I, Ceresi E, Faloia E, Wang S, Fortier M, Greenberg AS, Obin MS: Adipocyte death defines macrophage localization and function in adipose tissue of obese mice and humans. *J Lipid Res* 46:2347–2355, 2005
26. Pradhan AD, Manson JE, Rifai N, Buring JE, Ridker PM: C-reactive protein, interleukin 6, and risk of developing type 2 diabetes mellitus. *JAMA* 286:327–334, 2001
27. Boden G: Role of fatty acids in the pathogenesis of insulin resistance and NIDDM. *Diabetes* 46:3–10, 1997
28. Hotamisligil GS, Shargill NS, Spiegelman BM: Adipose expression of tumor necrosis factor-α: direct role in obesity-linked insulin resistance. *Science* 259:87–91, 1993
29. Uysal KT, Wiesbrock SM, Marino MW, Hotamisligil GS: Protection from obesity-induced insulin resistance in mice lacking TNF-α function. *Nature* 389:610–614, 1997
30. Yamauchi T, Kamon J, Waki H, Terauchi Y, Kubota N, Hara K, Mori Y, Ide

T, Murakami K, Tsuboyama-Kasaoka N, Ezaki O, Akanuma Y, Gavrilova O, Vinson C, Reitman ML, Kagechika H, Shudo K, Yoda M, Nakano Y, Tobe K, Nagai R, Kimura S, Tomita M, Froguel P, Kadowaki T: The fat-derived hormone adiponectin reverses insulin resistance associated with both lipoatrophy and obesity. *Nat Med* 7:941–946, 2001
31. Lazar MA: How obesity causes diabetes: not a tall tale. *Science* 307:373–375, 2005
32. Bastard JP, Maachi M, Van Nhieu JT, Jardel C, Bruckert E, Grimaldi A, Robert JJ, Capeau J, Hainque B: Adipose tissue IL-6 content correlates with resistance to insulin activation of glucose uptake both in vivo and in vitro. *J Clin Endocrinol Metab* 87:2084–2089, 2002
33. Senn JJ, Klover PJ, Nowak IA, Mooney RA: Interleukin-6 induces cellular insulin resistance in hepatocytes. *Diabetes* 51:3391–3399, 2002
34. Vozarova B, Weyer C, Hanson K, Tataranni PA, Bogardus C, Pratley RE: Circulating interleukin-6 in relation to adiposity, insulin action, and insulin secretion. *Obes Res* 9:414–417, 2001
35. Schreyer SA, Wilson DL, LeBoeuf RC: C57BL/6 mice fed high fat diets as models for diabetes-accelerated atherosclerosis. *Atherosclerosis* 136:17–24, 1998
36. Gao Z, Zuberi A, Quon MJ, Dong Z, Ye J: Aspirin inhibits serine phosphorylation of insulin receptor substrate 1 in tumor necrosis factor-treated cells through targeting multiple serine kinases. *J Biol Chem* 278:24944–24950, 2003
37. Lee JY, Sohn KH, Rhee SH, Hwang D: Saturated fatty acids, but not unsaturated fatty acids, induce the expression of cyclooxygenase-2 mediated through Toll-like receptor 4. *J Biol Chem* 276:16683–16689, 2001
38. Shi H, Kokoeva MV, Inouye K, Tzameli I, Yin H, Flier JS: TLR4 links innate immunity and fatty acid-induced insulin resistance. *J Clin Invest* 116:3015–3025, 2006
39. Murciano C, Villamon E, Gozalbo D, Roig P, O'Connor JE, Gil ML: Toll-like receptor 4 defective mice carrying point or null mutations do not show increased susceptibility to *Candida albicans* in a model of hematogenously disseminated infection. *Med Mycol* 44:149–157, 2006
40. Palliser D, Huang Q, Hacohen N, Lamontagne SP, Guillen E, Young RA, Eisen HN: A role for Toll-like receptor 4 in dendritic cell activation and cytolytic $CD8^+$ T cell differentiation in response to a recombinant heat shock fusion protein. *J Immunol* 172:2885–2893, 2004
41. Suganami T, Mieda T, Itoh M, Shimoda Y, Kamei Y, Ogawa Y: Attenuation of obesity-induced adipose tissue inflammation in C3H/HeJ mice carrying a Toll-like receptor 4 mutation. *Biochem Biophys Res Commun* 354:45–49, 2007
42. Poggi M, Bastelica D, Gual P, Iglesias MA, Gremeaux T, Knauf C, Peiretti F, Verdier M, Juhan-Vague I, Tanti JF, Burcelin R, Alessi MC: C3H/HeJ mice carrying a Toll-like receptor 4 mutation are protected against the development of insulin resistance in white adipose tissue in response to a high-fat diet. *Diabetologia* 50:1267–1276, 2007
43. Aguirre V, Werner ED, Giraud J, Lee YH, Shoelson SE, White MF: Phosphorylation of Ser^{307} in insulin receptor substrate-1 blocks interactions with the insulin receptor and inhibits insulin action. *J Biol Chem* 277:1531–1537, 2002
44. Gao Z, Hwang D, Bataille F, Lefevre M, York D, Quon MJ, Ye J: Serine phosphorylation of insulin receptor substrate 1 by inhibitor κB kinase complex. *J Biol Chem* 277:48115–48121, 2002
45. Senn JJ: Toll-like receptor-2 is essential for the development of palmitate-induced insulin resistance in myotubes. *J Biol Chem* 281:26865–26875, 2006
46. Song MJ, Kim KH, Yoon JM, Kim JB: Activation of Toll-like receptor 4 is associated with insulin resistance in adipocytes. *Biochem Biophys Res Commun* 346:739–745, 2006
47. Suganami T, Tanimoto-Koyama K, Nishida J, Itoh M, Yuan X, Mizuarai S, Kotani H, Yamaoka S, Miyake K, Aoe S, Kamei Y, Ogawa Y: Role of the Toll-like receptor 4/NF-κB pathway in saturated fatty acid-induced inflammatory changes in the interaction between adipocytes and macrophages. *Arterioscler Thromb Vasc Biol* 27:84–91, 2007